

Acoustic intensity near a high-powered military jet aircraft

Trevor A. Stout, Kent L. Gee, and Tracianne B. Neilsen

*Department of Physics and Astronomy, Brigham Young University, Provo,
Utah 84602, USA*
tstout@byu.edu, kentgee@byu.edu, tbn@byu.edu

Alan T. Wall

*Air Force Research Laboratory, Battlespace Acoustics Branch, Wright-Patterson AFB,
Dayton, Ohio 45433, USA*
alantwall@gmail.com

Michael M. James

Blue Ridge Research and Consulting, LLC, Asheville, North Carolina 28801, USA
michael.james@blueridgeresearch.com

Abstract: The spatial variation in vector acoustic intensity has been calculated between 100 and 3000 Hz near a high-performance military aircraft. With one engine of a tethered F-22A Raptor operating at military power, a tetrahedral intensity probe was moved to 27 locations in the geometric near and mid-fields to obtain the frequency-dependent intensity vector field. The angles of the maximum intensity region rotate from aft to sideline with increasing frequency, becoming less directional above 800 Hz. Between 100 and 400 Hz, which are principal radiation frequencies, the ray-traced dominant source region rapidly contracts and moves upstream, approaching nearly constant behavior by 1000 Hz.

© 2015 Acoustical Society of America

[SS]

Date Received: October 17, 2014 **Date Accepted:** May 14, 2015

1. Introduction

While modern high-power jet engines provide the thrust capability required by current-generation tactical military aircraft, they also produce high-amplitude sound fields. Jet noise is a significant contributor to military personnel hearing loss,¹ and there is interest in characterizing the sound from these engines to better address the problem. However, there are many difficulties inherent in the study of the supersonic, heated, turbulent jet engine exhaust. Typically, the sound field is characterized with acoustic pressure measurements. However, the vector acoustic intensity of the sound field contains both magnitude and directional information as a function of frequency, and thus, can provide additional insight into the nature of the sound sources in the turbulent mixing noise.

The application of vector intensity measurements to full-scale jet engine sound field characterization is unique. Acoustical measurements of high-performance jet engines are relatively rare,^{2,3} and the vector acoustic intensity, or measure of sound power flux, has had only limited application to primarily laboratory-scale jet noise analysis. Perhaps the most in-depth example of intensity analysis in aeroacoustics is that of Jaeger and Allen,⁴ who traced vectors from a two-dimensional intensity probe back toward the centerline of Mach 0.2–0.6 lab-scale jets, using the line intercepts to describe the source region. Intensity measurements have also been used in a lab-scale jet setting to verify the results from other inverse methods, such as beamforming.⁵ Recently, a three-dimensional intensity probe (the same one employed here) has been used to investigate the near field of solid rocket motor plumes, revealing the extended nature of the source region.^{6,7}

Relative to pressure measurements, even those utilizing array processing methods like holography or beamforming, acoustic intensity offers a direct description of the magnitude and direction of sound energy flow. The quantity, therefore, has potential to improve insights into jet noise features. Calculation of intensity requires knowledge of the pressure as well as acoustic particle velocity. Although specially manufactured sensors exist for particle velocity measurements,⁸ the high levels and potential for nonacoustic velocity fluctuations reduce the reliability of such sensors near a high-power jet. Alternatively, the established finite-difference method for approximating the particle velocity is based on closely spaced, phase and amplitude-matched microphones.

Results of using such an intensity probe in the vicinity of an F-22A Raptor are presented in this letter. A brief description of the experiment is followed by a summary of the method and spatial maps of the measured vector intensity as one engine was operated at military engine condition (the highest thrust condition below afterburner). A preliminary estimate of the maximum source location obtained via ray tracing the intensity vectors provides an example of the usefulness of this technique in characterizing jet noise sources.

2. Experiment

During 27–30 July 2009, a team of researchers from Blue Ridge Research and Consulting and Brigham Young University took measurements of the sound field of a tethered Lockheed Martin/Boeing F-22A Raptor. This effort represents the most extensive near-field acoustical study of a military aircraft to date. A rectangular, 90-microphone rig (used for other analyses) and attached three-dimensional intensity probe took data along two measurement planes at 4.1 and 5.6 m from the estimated shear layer, and along a 22.9-m radius arc, to the sideline and aft of the aircraft.⁹ The F-22 was tethered to a concrete run-up pad surrounded on either side by rain-packed dirt (see Fig. 1). The engine nozzles' centerline was 1.91 m above the ground. One of the two engines was held at idle, while the other was incrementally fired at one of four engine conditions: idle, intermediate (~80% throttle), military (full throttle), and full afterburner. In this letter, results for military engine condition are presented, with data synchronously acquired at a sampling frequency of 96 kHz.

The probe was located on top of the 90-microphone array, which took measurements in 2.3 m increments along the measurement planes, and at three different heights. For each data location, the probe and rig were fixed while the engine ramped up to one of the engine conditions. The probe was oriented such that one edge of the probe's tetrahedral frame was parallel with the approximate shear layer. For the results presented in this letter, the center of the intensity probe was located at a height of approximately 2.54 m. In the following figures, the z axis is defined as the jet exhaust



Fig. 1. (Color online) Measurement setup with static engine firing (left), and close-up of microphone rig and intensity probe (right). The rig and probe were mounted to an aluminum guide rail to ensure accuracy of the measurement plane geometries.

centerline, with the x axis horizontal and perpendicular to it, according to a right-handed coordinate system. For the proceeding figures, the point at $z=0$ and $x=0$ is defined as the active jet nozzle exit, and angles are defined from the engine inlet, relative to the jet centerline.

For the measurement planes and arc, 27 individual measurements were performed to collect the data presented in this letter (10 locations per plane and 7 along the arc). Some nonstationarity is to be expected because of the uncertainty in a scan-based measurement taken over multiple run-ups. To quantify this uncertainty, 50 reference microphones⁹ arranged parallel to the jet centerline, located between $z=-3$ m and $z=28$ m at $x=11.6$ m, with 0.61 m spacing, provide baseline pressure levels for the intensity probe's first 20 measurement positions. Comparison of the pressure levels recorded by this reference array for the static engine firings quantifies the variability between run-ups. Figure 2 shows the average overall sound pressure level (OASPL) at the reference microphones, whose locations span the entire range of intensity probe locations along the z axis. Error bars indicate the standard deviation in squared pressure over the run-ups. In Fig. 2, there is small variation across the 30 m aperture, with typical standard deviations of 1 dB or lower. The spatial average of the standard deviations, across all the reference microphones, is 0.4 dB. Thus, although the F-22 run-ups do not represent a perfectly repeatable source, the uncertainty is small enough that measurements from various run-ups, corresponding to different intensity probe locations, may be combined to form a map of the F-22 sound field.

The intensity probe had the same configuration used in the near-field rocket studies in Refs. 6 and 7. The external tetrahedral frame held four low-sensitivity GRAS 40BD prepolarized microphones with 26CB preamplifiers at a constant separation distance, facing inward, such that their diaphragms could be circumscribed by a 1.5 in. diameter sphere. In laboratory tests of this probe configuration in anechoic conditions up to 2 kHz, intensity values had <1 dB maximum error in magnitude, and <10° direction error.¹⁰

3. Methods and results

To calculate intensity vectors from the pressure measurements, the finite-difference approximation (or p-p) method¹¹ was used. In the frequency domain, the single-sided, active intensity component between two microphones along the axis connecting the two microphones is given by

$$I(\omega) = \frac{-1}{\rho_0 \omega d_{XY}} \text{Im}\{G_{XY}(\omega)\},$$

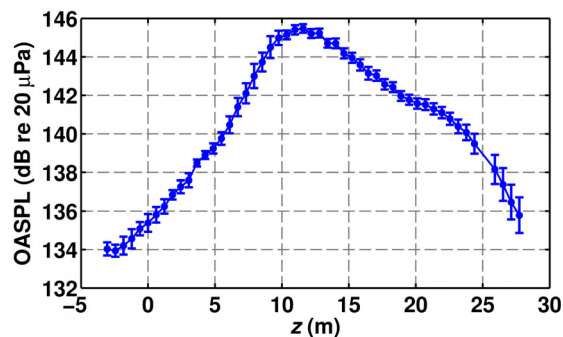


Fig. 2. (Color online) Average OASPL vs downstream distance at military power, for the 50 reference microphones at 11.6 m from the centerline, with standard deviation among 27 individual run-ups indicated by error bars. Three microphones near $z=27$ and 13 m had failing power supplies for several run-ups; these data were removed before averaging. The average standard deviation across all reference microphones is 0.4 dB.

where d_{XY} is the distance between the two microphones, G_{XY} is their single-sided cross-spectrum, ω is the frequency of interest, and ρ_0 the ambient fluid density. To calculate the intensity in three dimensions, the cross-spectra between the four microphones in the intensity probe were weighted and summed according to a least-squares method developed by Pascal and Li¹² and recently implemented by Wiederhold *et al.*¹³ The data were time-averaged over the full length of each static engine firing, about 25 s.

Intensity values at one-third-octave band center frequencies of 125, 160, 250, 315, 500, and 1250 Hz are shown in Fig. 3, with frequency bin widths of 5.9 Hz. Only the horizontal (x - z) intensity components are displayed. For this figure, the linear internal scaling used by the rendering program to define vector lengths is kept consistent, while intensity magnitudes are cube-root scaled for convenience in visualization. Sound intensity level (SIL) values, as shown by the color bars, are unscaled. A movie displaying intensity data at additional frequencies in the range from 125 to 1250 Hz is available (see Mm. 1).

Mm. 1. F22 Intensity. This is a file of type “mp4” (1.7 Mb).

Study of the intensity vector maps elucidates the frequency-dependent nature of the F-22 sound field. Along measurement planes 1 and 2, the location of peak intensity shifts upstream as frequency increases. Table 1 specifies the intensity probe

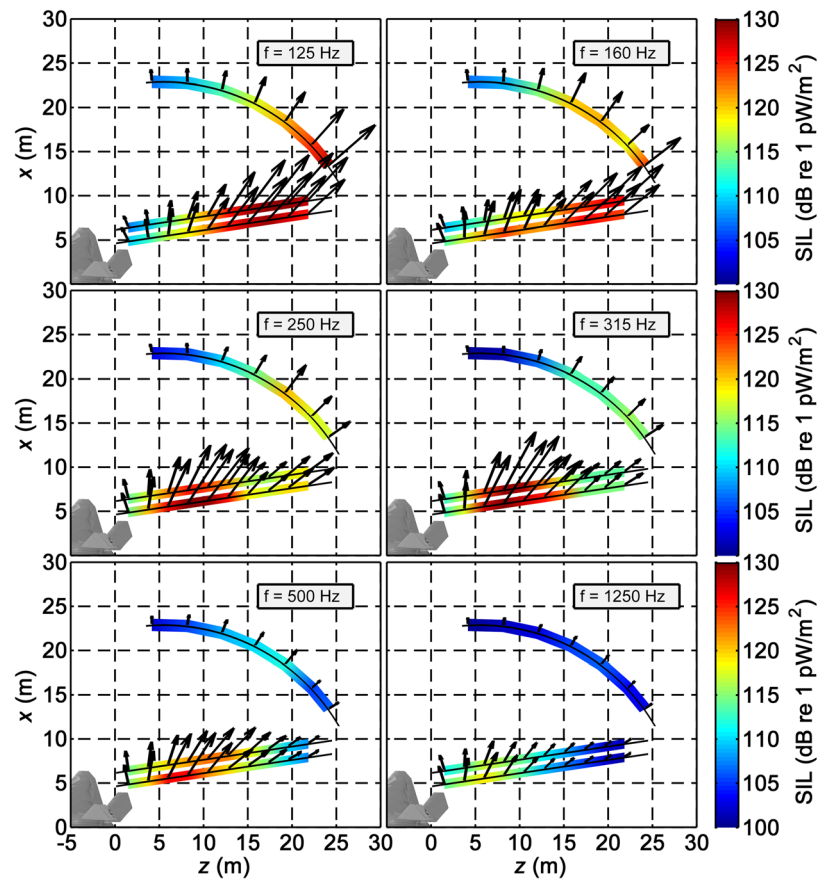


Fig. 3. (Color online) Intensity at military condition for select one-third octave band center frequencies. The intensity probe was located at the base of each vector arrow. Note how the region of maximum intensity shifts upstream with increasing frequency, while the overall sound intensity level decreases. A movie displaying these data at 36 frequencies from 125 to 1250 Hz is available online.

Table 1. Extent of measurement regions where SIL is 3 dB or less from the maximum along measurement plane 2, at military power for select one-third-octave band center frequencies.

	125 Hz	160	200	250	315	500	800	1250
Range upstream	$z = 15.1$ m	17.3	8.3	8.3	8.3	8.3	8.3	6.0
Downstream	$z = 21.8$ m	21.8	21.8	10.5	10.5	12.8	10.5	8.3

locations along the z axis where the SIL is within 3 dB of the maximum SIL along plane 2 at one-third octave band center frequencies. The intensity also decreases in magnitude at higher frequencies, as expected from a jet power spectrum. The region of maximum intensity exhibits strong directionality at low frequencies: compare the narrower directionality at 125 Hz to the wider spread of vector directions at 1250 Hz. Another interesting feature is seen at 160 Hz, where there appear to be two separate regions of high-magnitude intensity with different directionality near $z=8$ m and $z=20$ m downstream,¹⁴ corresponding to two prominent radiation lobes at or near this frequency.¹⁵ Additional investigations into these phenomena are ongoing,¹⁶ but outside the scope of this letter.

The presence of ground reflections from the concrete pad and rain-packed dirt has a noticeable effect on the data. At 125 Hz, intensity vectors in the maximum intensity region along measurement plane 2 near $z=20$ m have magnitudes about 1.5 dB higher than those along plane 1. This is contrary to expectations based on geometric spreading and is due to the interference of direct and reflected signals. The presence of ground reflection interference is readily observed in the level-based planar measurements from the 90-microphone array.¹⁷

As a straightforward method to approximate the frequency-dependent source region, intensity vectors at the measurement plane 5.6 m to the side of the shear layer are traced back to the jet centerline. This technique is prompted by the methods of Jaeger and Allen in studying subsonic jets.⁴ However, because of the extended nature of the source, rather than use the intersection of the ray-traced lines from all measurement locations, only those with SIL within 3 dB of the maximum along measurement plane 2 are used at each frequency; this region is termed the “3 dB-down region.” Vectors within the 3 dB-down region are traced backwards, so that the left-most and right-most intercepts along the jet centerline define an approximate peak source region. This estimated source region is shown in Fig. 4 for one-third-octave band center frequencies between 100 and 3000 Hz. The generalized source region is shown to contract

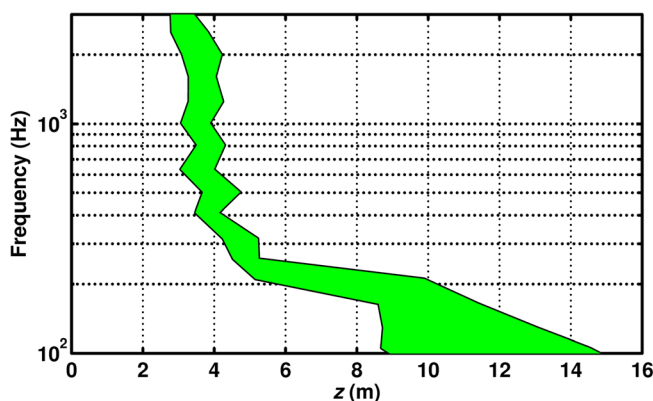


Fig. 4. (Color online) Generalized source region for military condition, found by tracing intensity vectors back from the 3 dB-down region along measurement plane 2. Data is presented at one-third octave band center frequencies between 100 Hz and 3 kHz.

and move upstream with increasing frequency. The source location shifts rapidly between 100 and 400 Hz, moving from about 9–15 m downstream to 3.5–4.5 m downstream. Above this frequency, the source region indicated in Fig. 4 centers at about 4 m downstream. The slight variations above 400 Hz are likely due to the uncertainty in choosing discrete intensity vectors in the 3 dB-down region with sparse data locations.

Source distributions found using beamforming and holography methods with the same F-22 measurements agree with the source location trends shown in Fig. 4, although there is some variation among the methods in exact source locations. Beamforming from the ground-based array of microphones (steered to the jet centerline) finds that the source region centers at 6 m downstream at 100 Hz, and contracts and centers at approximately 3 m downstream at 500 Hz.¹⁸ Cylindrical near-field acoustical holography (using the ground-based array) reconstructs a source distribution along the shear layer (instead of the jet centerline) centered at about 7 m downstream at 100 Hz, and at 5 m downstream at 250 Hz.¹⁵ Similarities and differences in source distributions among the various methods require additional investigation with benchmark cases to determine factors that affect the ability of the methods to produce consistent results. In addition, a more detailed comparison needs to be completed to determine how the estimated source region varies with frequency and engine condition.

The source location trends in Fig. 4 can also be qualitatively compared with prior source reconstructions from jets of different scales and conditions. Laboratory-scale beamforming studies (for example, Refs. 19 and 20) indicate that the extended source region from laboratory-scale jets contracts and moves upstream with increasing frequency. Although the results presented in this letter from the F-22 intensity measurements agree with this general trend, the rapidity of transition in source location from 100 to 400 Hz is not seen in typical laboratory-scale studies. However, Lee and Bridges¹⁹ found that an increase in jet velocity for their heated subsonic jet resulted in a more abrupt transition in source location with frequency above a Strouhal number of 0.5. Further increases in Mach number to approach full-scale military jet conditions could feasibly change the transition region to be more similar to the behavior in Fig. 4, but this requires additional investigation. Notably, the beamforming analysis of Schlinker *et al.*² on a high-performance aircraft engine predicts that the source region does not vary significantly with increasing frequency. This discrepancy may be due to the fact that the data used were high-pass filtered at 200 Hz, while data at or below 200 Hz are necessary to see the rapid transition in the F-22 sound source region shown in Fig. 4. As a final observation, the extended source region presented here is more compact than the intensity-based source region found previously for a GEM-60 solid rocket motor⁶ and is significantly more extended than Jaeger and Allen's⁴ subsonic, unheated jets.

4. Conclusion

The usefulness of near-field acoustic intensity analysis for full-scale jet aeroacoustic source characterization is demonstrated in this letter. Preliminary intensity estimates from full-throttle static engine firings of an F-22A Raptor have been made from 100 to 3000 Hz, and maps are presented between 125 and 1250 Hz. A ray-tracing method predicts the peak source location and extent as a function of frequency. Future work will involve a more detailed analysis of the F-22 sound field as a function of engine condition, and in a wider frequency range using alternate intensity processing methods.²¹ It would also be beneficial if comparison with the intensity fields near other scales of jets and with similar heated, supersonic conditions were made possible by future studies involving intensity measurements.

Acknowledgments

The authors gratefully acknowledge funding for this analysis from the Office of Naval Research. The measurements were funded by the Air Force Research Laboratory through

the SBIR program and supported through a Cooperative Research and Development Agreement (CRDA) between Blue Ridge Research and Consulting, Brigham Young University, and the Air Force. Distribution A: Approved for public release; distribution unlimited. Cleared 09/23/2014; 88ABW-2014-4495.

References and links

- ¹K. L. Gee, T. B. Neilsen, A. T. Wall, J. M. Downing, and M. M. James, “The ‘sound of freedom’: Characterizing jet noise from high-performance military aircraft,” *Acoust. Today* **9**(3), 8–21 (2013).
- ²R. H. Schlinker, S. A. Liljenberg, D. R. Polak, K. A. Post, C. T. Chipman, and A. M. Stern, “Supersonic jet noise source characteristics and propagation: Engine and model scale,” AIAA paper No. 2007-3623.
- ³B. Greska and A. Krothapalli, “On the far-field propagation of high-speed jet noise,” in *Proceedings of ASME 2008 Noise Control and Acoustics Division Conference*.
- ⁴S. M. Jaeger and C. S. Allen, “Two-dimensional sound intensity analysis of jet noise,” AIAA paper No. 93-4342 (1993).
- ⁵S. R. Ventakesh, D. R. Poak, and S. Narayana, “Beamforming algorithm for distributed source localization and its application to jet noise,” *AIAA J.* **41**, 1238–1246 (2003).
- ⁶K. L. Gee, J. H. Giraud, J. D. Blotter, and S. D. Sommerfeldt, “Near-field vector intensity measurements of a small solid rocket motor,” *J. Acoust. Soc. Am.* **128**, EL69–EL74 (2010).
- ⁷K. L. Gee, J. H. Giraud, J. D. Blotter, and S. D. Sommerfeldt, “Energy-based acoustical measurements of rocket noise,” AIAA paper No. 2009-3165 (2009).
- ⁸R. Raangs, W. F. Druyvesteyn, and H. E. De Bree, “A low-cost intensity probe,” *J. Audio Eng. Soc.* **51**(5), 344–357 (2003).
- ⁹A. T. Wall, K. L. Gee, M. M. James, K. A. Bradley, S. A. McNerny, and T. B. Neilsen, “Near-field noise measurements of a high-performance jet aircraft,” *Noise Control Eng. J.* **60**, 421–434 (2012).
- ¹⁰J. H. Giraud, “Experimental analysis of energy-based acoustic arrays for measurement of rocket noise fields,” M.S. thesis, Brigham Young University (2013).
- ¹¹F. Fahy, *Sound Intensity* (CRC Press, Boca Raton, FL, 2002), p. 97.
- ¹²J.-C. Pascal and J.-F. Li, “A systematic method to obtain 3D finite-difference formulations for acoustic intensity and other energy quantities,” *J. Sound Vib.* **310**, 1093–1111 (2008).
- ¹³C. P. Wiederhold, K. L. Gee, J. D. Blotter, S. D. Sommerfeldt, and J. H. Giraud, “Comparison of multi-microphone probe design and processing methods in measuring acoustic intensity,” *J. Acoust. Soc. Am.* **135**(5), 2797–2807 (2014).
- ¹⁴T. A. Stout, K. L. Gee, T. B. Neilsen, A. T. Wall, and M. M. James, “Intensity analysis of the dominant frequencies of military jet aircraft noise,” *Proc. Mtgs. Acoust.* **20**, 040010 (2014).
- ¹⁵A. T. Wall, K. L. Gee, T. B. Neilsen, D. W. Krueger, and M. M. James, “Cylindrical acoustical holography applied to full-scale military jet aircraft noise,” *J. Acoust. Soc. Am.* **136**, 1120–1128 (2014).
- ¹⁶T. B. Neilsen, K. L. Gee, and M. M. James, “Spectral characterization in the near and mid-field of military jet aircraft noise,” AIAA paper No. 2013-2191 (2013).
- ¹⁷J. Morgan, T. B. Neilsen, K. L. Gee, A. T. Wall, and M. M. James, “Simple-source model of high-power jet aircraft noise,” *Noise Control Eng. J.* **60**, 435–449 (2012).
- ¹⁸B. M. Harker, K. L. Gee, T. B. Neilsen, A. T. Wall, and M. M. James, “Phased-array measurements of full-scale military jet noise,” AIAA paper No. 2014-3069 (2014).
- ¹⁹S. S. Lee and J. Bridges, “Phased-array measurements of single flow hot jets,” AIAA paper No. 2005-2842 (2005).
- ²⁰D. Papamoschou and A. Dadvar, “Localization of multiple types of jet noise sources,” AIAA paper No. 2006-2644 (2006).
- ²¹D. C. Thomas, B. Y. Christensen, and K. L. Gee, “Phase and amplitude gradient method for the estimation of acoustic vector quantities,” *J. Acoust. Soc. Am.* **137**, 3366 (2015).